

The first two years of measurements were subjected to consistency problem due to an inconsistency between two different measurement scenarios or observation deficiencies. We performed the optical alignment evaluation, the surface pressure and timing error corrections, as well as the detector consistency to ensure that the retrievals are consistent throughout the entire measurement period.

1. Description of our IFS125HR

The FTS 125HR has six detectors, four beam splitters, and nine optical compartments which corresponds to a maximum optical path difference (OPD) of 937.5 cm. All detector and beam splitter types, as well as their work ranges are listed in Table S1 and S2. The spectrometer covers a spectral range from 420 cm^{-1} to 50,000 cm^{-1} . The solar tracker is mounted on a platform inside a dome which is made up of two spherical caps. The dome protects the solar tracker from bad weather such as rain, snow and strong wind. The rotation of the dome and the open-close state of the two spherical caps are controlled by three individual motors. The solar tracker follows the sun by adjusting two aluminized folding mirrors and guides the sunlight into the FTS spectrometer. A tracking precision of 0.1° can be achieved by using the Camtracker mode. The weather station mounted near the dome includes sensors for air pressure (± 0.1 hPa of precision), air temperature ($\pm 0.1^\circ\text{C}$), relative humidity ($\pm 1\%$), solar radiation ($\pm 10\%$, short wave), wind speed, wind direction, and the presence of rain, snow, or heavy dew. The IFS125HR system is equipped with a multi-stage scroll pump to keep the spectrometer under vacuum when taking measurements. The vacuum condition can enhance the stability of the system.

Table S1. Detector type

Detector	Spectral range (cm^{-1})	Operating temperature
GaP diode	50,000 ~ 18,000	Room temperature
vacuum diode	43,000 ~ 24,000	Room temperature
Si diode	25,000 ~ 9,000	Room temperature
Extended InGaAs	12,800 ~ 4,000	Room temperature
InSb	11,000 ~ 1,850	Liquid-nitrogen cooled
MCT broad band	12,000 ~ 420	Liquid-nitrogen cooled

Table S2. Beam splitter type

Beam splitter	Measurement range	Suitable detectors	Spectral range (cm ⁻¹)
KBr	MIR	MCT, InSb	4,800 - 450
CaF ₂	NIR	InSb, InGaAs, Si	14,000 - 1,850
Quartz (II)	Visible	Si	25,000 - 9,500
Quartz UV	UV	Gap, Vacuum diode	43,000-28,000

2. Observation activities

The instrument has operated almost continuously since July 2014, however data gaps occurred due to an instrument mechanical problem between December 2014 and February 2015. Before 27 July 2015, only the near-infrared (NIR) solar spectra were acquired. After that, we have the facilities to run NDACC-IRWG (Network for Detection of Atmospheric Composition Change - Infrared Work Group, <http://www.ndacc.org/>) observations, the NIR and mid-infrared (MIR) solar spectra were alternately acquired in routine observation. The NIR spectra provide highly precise and accurate column-averaged abundances for CO₂, CH₄, N₂O, CO, HF, H₂O, and HDO. In contrast, the MIR spectra are used to retrieve time series of mixing ratio profiles for O₃, HNO₃, HCl, HF, CO, N₂O, CH₄, HCN, C₂H₆, ClONO₂ and other gases, e.g., H₂O, HDO/ H₂O ratio, OCS or NH₃.

3. Consistency evaluation and corrections

Since all measurements were not taken with the same measurement settings, consistency evaluation and technical corrections were performed to ensure the retrievals are consistent throughout the entire measurement period.

3.1 Optical alignment evaluation

In order to accurately retrieve the total column abundances, a good alignment of the FTIR is crucial (Hase et al., 2013). The instrument line shape (ILS) retrieved from HCl gas cell measurements is a useful indicator of the FTIR's alignment (Hase et al., 1999). The ILS calculations were performed with the LINEFIT 14.5 software. For the measurements in this study, two major factors may result in retrieval bias via altering ILS. First, we did not perform alignment for more than one year due to the lack of facilities, while the ILS may drift slowly due to mechanical degradation over time

(Hase et al., 2012). Second, different entrance aperture and detector were used before and after 27 July 2015, which may cause different ILS (Sun et al., 2017). In addition, the ILS measurements are commonly performed using an internal lamp. For the gas measurements, the ILS of the whole system (i.e. including the solar tracking system and the entrance optics) is of utmost importance. Hase et al. (1999) and Sun et al. (2017) have shown that the ILS characteristics derived from lamp and sun spectra are in good agreement. However, this is dependent on instrument.

To quantify all these influences, the ILS results derived from lamp spectra with InSb & 0.5 mm aperture and InGaAs & 1 mm aperture were compared with the ILS derived from sun spectrum with InGaAs & 1 mm aperture. The comparison is shown in Fig. S1. The modulation efficiencies (MEs) and phase errors (PEs) of the three scenarios exhibit a little difference. Nevertheless, all MEs vary from the ideal value of 1.0 by less than 2 % and PEs are less than 0.02 rad, which Hase et al. (1999) considered as a good alignment. Therefore, the retrieval bias caused by ILS error is of secondary importance.

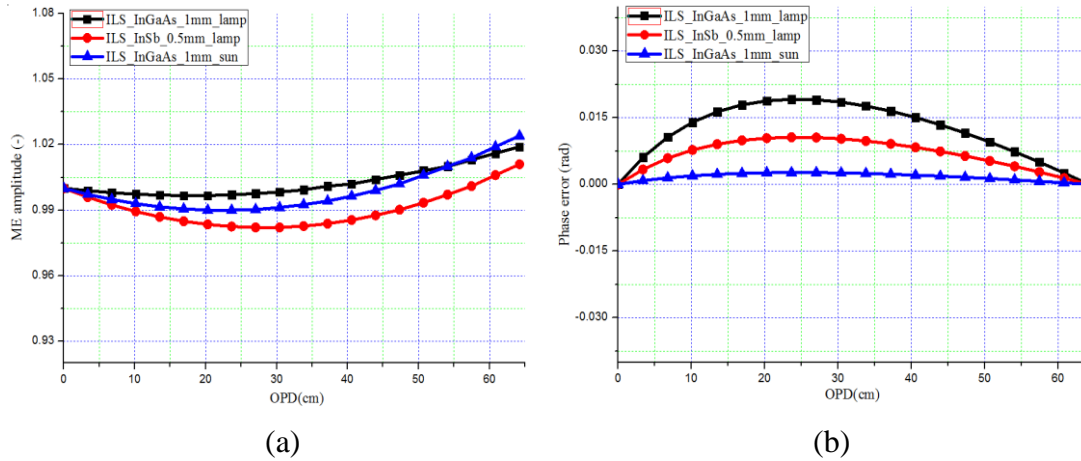


Figure S1. The ILS results derived from lamp spectra with InSb & 0.5mm aperture (red line) and InGaAs & 1mm aperture (black line), and sun spectrum with InGaAs & 1mm aperture (blue line). (a) and (b) represent the ME amplitude and phase error, respectively.

3.2 Surface pressure correction

Surface pressure is used to derive the site pressure - altitude for each spectrum in the retrieval. Thus, the surface pressure measurements should be known with sufficient accuracy to avoid retrieval bias. An underestimated surface pressure would cause an underestimated X_{gas} , and an overestimated surface pressure would cause an

overestimated X_{gas} . The largest pressure error permitted by the TCCON data protocol is ± 1 hPa. The measurements in this study lacked dedicated surface pressure data until the weather station started to record meteorological data in September 2015. To avoid the pressure related biases, the synchronized meteorological data obtained from a nearby weather station (about 1 km away) were applied for the measurements before September 2015. The pressure sensors in both weather stations are calibrated periodically against a mercury manometer. All pressures were converted to an altitude where the first mirror of the solar tracker locates through

$$P_{\text{obs}} = P_{\text{pre}} \times \exp(-9.83 \times \text{alt_diff} / (287 \times (T_{\text{pre}} + 273.15))), \quad (1)$$

$$\text{alt_diff} = (\text{obs_alt} \times 1000) - \text{pre_alt}, \quad (2)$$

where obs_alt (unit of km) and pre_alt (unit of m) represent the altitude of the solar tracker and the pressure sensor, respectively. The alt_diff (unit of m) is the altitude difference between the solar tracker and the pressure sensor. P_{pre} (unit of mb) and T_{pre} (unit of °C) represent the pressure and temperature at the altitude of the pressure sensor, respectively, and P_{obs} (unit of mb) represents the pressure at the altitude of the solar tracker.

3.3 Timing error correction

The timestamp assigned to each spectrum is used to derive the measurement SZA. Timing error would cause SZA error and hence result in retrieval bias. The measurements in this study could be subjected to timing errors before 2 January 2015. A timing error is characterized by a large and asymmetric diurnal variation of X_{air} when the surface pressure is accurate and spectra with no laser sampling error and in good alignment. We assume that the daily timing error is a constant and it drifts linearly with time. Consequently, the timing error can be corrected iteratively by adding or subtracting a step value until the diurnal variation of retrieved X_{air} is less than 1 % and symmetric. Fig.S2 and Fig.S3 show the retrieved X_{air} diurnal variation without and with the time correction scheme, respectively. The spectra were recorded on a typical clear day on 24 October 2014. Before timing error correction, the daily X_{air} varies more than 4 % over a large range from 0.96 to 1.04. Whereas after

correction by a minus of 65s in the retrieval, the daily X_{air} concentrates on 0.984 and varies less than 1 %, which is within the requirements of the TCCON data protocol. The timing error correction scheme was used for other measurements with timing errors.

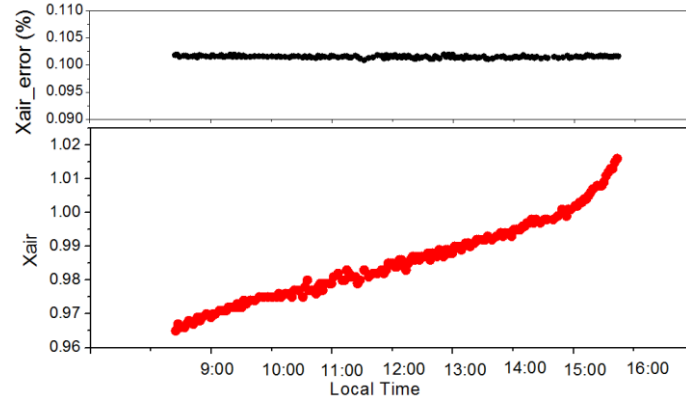


Figure S2 X_{air} diurnal variations retrieved from the spectra recorded on a typical clear day on 24 October 2014. A timing error is obviously, the daily X_{air} varies more than 4% over a large range from 0.96 to 1.04. The top and bottom panel are time series of fitting uncertainties and X_{air} amounts, respectively.

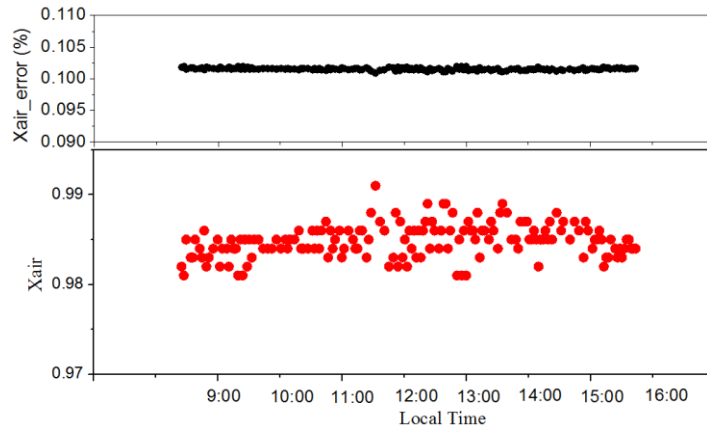


Figure S3 X_{air} diurnal variations after correcting a timing error of -65s to Fig.S2. The daily X_{air} concentrates on 0.984 and varies less than 1%, which is within the requirements of the TCCON data protocol. The top and bottom panel are time series of fitting uncertainties and X_{air} amounts, respectively.

3.4 Consistency between InSb and InGaAs detector

InSb is a LN₂-cooled and easily saturated detector, whereas InGaAs operates under room temperature and does not normally saturate under our measurement conditions. Different properties of these two detectors may result in biases between the measurements before and after 27 July 2015 even though Section 3.1 in this

supplement verified that InSb & 0.5 mm aperture and InGaAs & 1 mm aperture provide similar ILSs. To examine the consistency between the InSb and InGaAs detectors, the InSb & 0.5 mm aperture and InGaAs & 1 mm aperture were used alternatively to record solar spectra on a clear day on 1 April 2016. Fig. S4 shows typical spectra recorded with the InSb and InGaAs detectors. The spectral response of the two detectors are different. The discrepancies in O₂ window are larger than those in CO₂ window. We performed five groups of alternative measurements, and each group measurement includes 8 InSb spectra and 8 InGaAs spectra.

The retrieved XCO₂ time series are shown in Fig.S5. The XCO₂ time series derived from InSb & 0.5 mm aperture are 1.991 ppm lower than those derived from InGaAs & 1mm aperture. In order to determine the cause of these biases, the retrieved O₂ and CO₂ total columns between different detectors were compared. Fig.S6 shows total columns of CO₂ in each window for different detectors. Fig.S7 shows the window averaged total columns of CO₂ and O₂. Table S3 lists statistical biases between the measurements with InSb & 0.5 mm aperture and InGaAs & 1 mm aperture. The results show that the O₂ window has a large bias ~0.6 % for InSb & 0.5mm aperture compared with InGaAs & 1 mm aperture. The bias in each CO₂ window is much smaller, with mean biases of 0.129 %.

We conclude that different detectors result in large bias in O₂ total column and slightly biases in CO₂ total columns, and thus cause the biases in XCO₂. To avoid the systematic biases, the additive offsets of 1.991 ppm was applied to all XCO₂ time series before 27 July 2015, provided that these biases are consistent throughout the entire measurement period. Similar additive offsets were also performed for other gases such as CH₄, CO, N₂O, HF, H₂O and HDO.

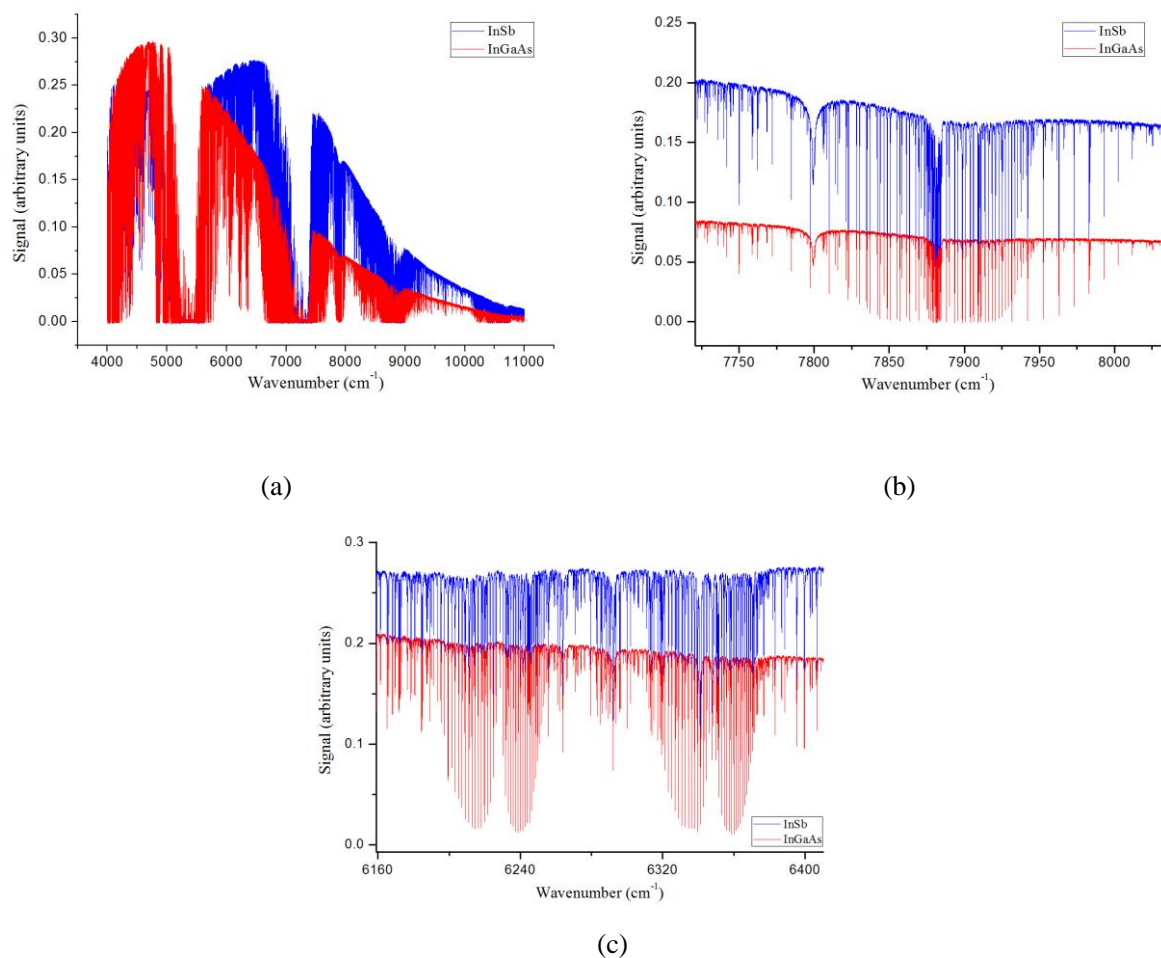


Figure S4. (a) Typical solar spectra recorded by the Hefei InSb and InGaAs detector. The two spectra were recorded within a close interval on a clear day on 1 April 2016. (b) Expanded view of the O₂ window from the same spectra. (c) Expanded view of the CO₂ window from the same spectra.

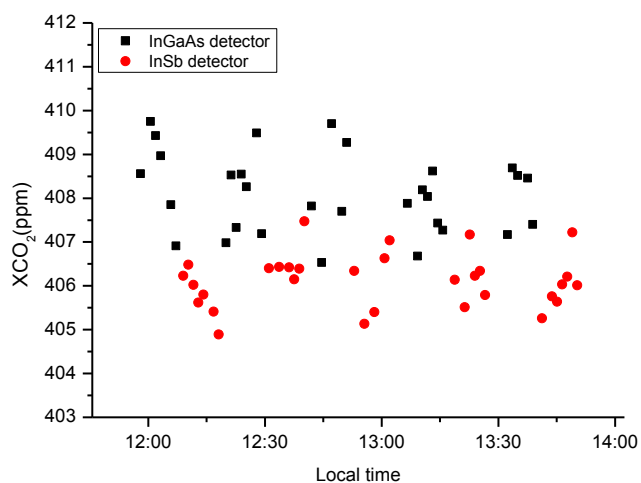


Figure S5 XCO₂ time series derived from spectra recorded with different detectors. The black dots and red dots represent the results derived from Hefei InGaAs and InSb spectra, respectively. The InSb and InGaAs spectra were recorded alternatively. Five groups of alternative measurements are performed.

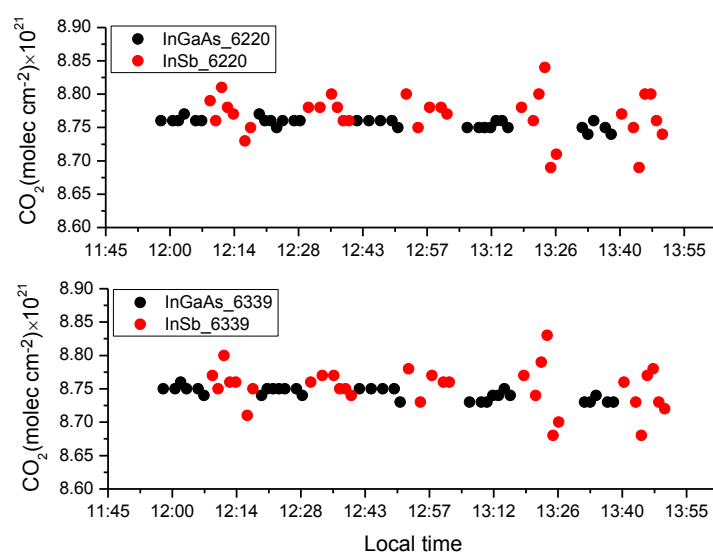


Figure S6 Total columns of CO₂ in each window that derived from spectra recorded with different detectors. The black dots and red dots represent the results derived from Hefei InGaAs and InSb spectra, respectively. The InSb and InGaAs spectra were recorded alternatively. Five groups of alternative measurements are performed.

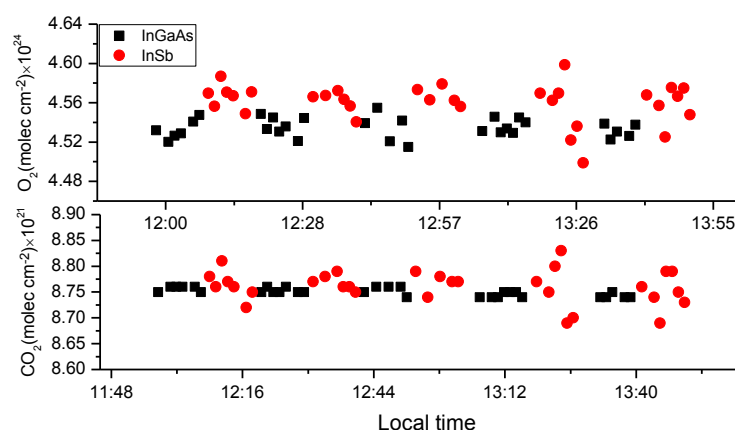


Figure S7 The window averaged total columns of O₂ and CO₂ derived from spectra recorded with different detectors. The black dots and red dots represent the results derived from Hefei InGaAs and InSb spectra, respectively. The InSb and InGaAs spectra were recorded alternatively. Five groups of alternative measurements are performed.

Table S3 Statistical biases between the measurements with InSb & 0.5mm aperture and InGaAs & 1mm aperture. The InGaAs & 1mm aperture is taken as the reference

Gases	Windows (cm ⁻¹)	Total column bias (molec×cm ⁻²)	Relative bias (%)	DMF offset (ppm)	Correction factor (ppm)
O ₂	7885	0.027×10 ²⁴	0.605	0 ^(*)	0 ^(*)
CO ₂	6220	0.012×10 ²¹	0.138	1.991	1.991
	6339	0.01×10 ²¹	0.110		
	Window averaged	0.011×10 ²¹	0.129		

*The DMF of O₂ is assumed to be a constant of 0.2095 in the GFIT retrieval, thus no correction factor is used for O₂ results.

References

- Hase, F., Blumenstock, T., and Paton-Walsh, C.: Analysis of the instrumental line shape of high resolution Fourier transform IR spectrometers with gas cell measurements and new retrieval software, *Appl. Optics*, 38, 3417–3422, doi:10.1364/AO.38.003417, 1999.
- Hase, F.: Improved instrumental line shape monitoring for the ground-based, high-resolution FTIR spectrometers of the Network for the Detection of Atmospheric Composition Change, *Atmos. Meas. Tech.*, 5, 603–610, doi:10.5194/amt-5-603-2012, 2012.
- Hase, F., Drouin, B. J., Roehl, C. M., Toon, G. C., Wennberg, P. O., Wunch, D., Blumenstock, T., Desmet, F., Feist, D. G., Heikkinen, P., De Mazière, M., Rettinger, M., Robinson, J., Schneider, M., Sherlock, V., Sussmann, R., Tóth, Y., Warneke, T., and Weinzierl, C.: Calibration of sealed HCl cells used for TCCON instrumental line shape monitoring, *Atmos. Meas. Tech.*, 6, 3527–3537, doi:10.5194/amt-6-3527-2013, 2013.
- Sun, Y., Palm, M., Weinzierl, C., Petri, C., Notholt, J., Wang, Y., and Liu, C.: Technical note: Sensitivity of instrumental line shape monitoring for the ground-based high-resolution FTIR spectrometer with respect to different optical attenuators, *Atmos. Meas. Tech.*, 10, 989–997, <https://doi.org/10.5194/amt-10-989-2017>, 2017.